Molecular Biology, Vol. 33, No. 2, 1999, pp. 180–187. Translated from Molekulyarnaya Biologiya, Vol. 33, No. 2, 1999, pp. 214–222.

BIOPOLYMER PHYSICS AND PHYSICAL CHEMISTRY

UDC 577.152.314:57.012.7

Extracellular Endonuclease of *Serratia marcescens*. 1. Three-Dimensional Structure of Crystalline Protein at 1.7 Å Resolution

V. Yu. Lunin[1], E. V. Blagova[2], V. M. Levdikov[2], V. V. Lunin[2], S. V. Shlyapnikov[3], M. Perbandt[4], K. S. Raishankar[4], H. Betzel[4], and A. M. Mikhailov[2]

[1] *Institute of Mathematical Problems in Biology, Russian Academy of Sciences, Pushchino, Moscow Region, 142292 Russia*
[2] *Shubnikov Institute of Crystallography, Russian Academy of Sciences, Moscow, 117333 Russia; E-mail: amm@biostr.crystal.msk.ru*
[3] *Engelhardt Institute of Molecular Biology, Russian Academy of Sciences, Moscow, 117984 Russia*
[4] *Institute of Physiological Chemistry, Hamburg University, Hamburg, 22603 Germany*

Received February 16, 1998

Abstract—A refined crystal structure of *Serratia marcescens* nuclease is reported to an *R* factor of 17.3% and R_{free} factor of 22.2% at a 1.7 Å resolution. The structure includes 3678 nonhydrogen atoms of the enzyme and 443 bound water molecules. The average deviations of bond lengths and valent angles from their standard values are 0.011 Å and 1.8°, and the maximal deviations are 0.07 Å and 11°, respectively. A new topological model of the enzyme molecule is proposed, indicating high symmetry of the monomer in its N- and C-terminal regions.

Key words: *Serratia marcescens*, extracellular endonuclease, X-ray crystallography, atomic structure

INTRODUCTION

The extracellular endonuclease of *S. marcescens* (*Sm* nuclease, EC 3.1.4.9) belongs to a family of structurally related nucleodepolymerases, which split the 3'O-P phosphodiester bond in single- and double-stranded DNA and RNA to form 5'-phosphorylated oligonucleotides, and are nonspecific with respect to the carbohydrate moiety of the nucleic acids [1–5].

At least three isoforms of *Sm* nuclease, which differ somewhat in their N-terminal structures, are known to date: *Sm* 1, *Sm* 2, and *Sm* 3. They apparently arise by enzymatic proteolysis of the native "mature" molecule in the periplasmic space or during transport across the cytoplasmic membrane [6, 7]. Isoforms *Sm* 1 and *Sm* 3 differ from the parent nuclease *Sm* 2 in lacking respectively three or one N-terminal amino acid residue.

Studies of the three-dimensional crystal structure of *Sm* nuclease were initiated nearly concurrently by us [8, 9] and a group at the University of Houston [10]. Later, Miller *et al.* [11], using isomorphous replacement, have obtained a refined structure of *Sm* nuclease at 2.1 Å (29,466 reflections). According to this structure, the protein molecule can be divided, as a first approximation, into three regions: a central β-sheet formed by six antiparallel β-strands, which is flanked by an α/β domain (three short α-helices and a β-sheet of two antiparallel β-strands) on one side and a conformational domain (long irregular loops and one extended α-helix) on the other.

Here we describe a refined crystal structure of *Sm* nuclease at 1.7 Å (57,000 reflections), which provides more accurate and reliable information on the protein tertiary structure. A new topological model proposed for the polypeptide chain allows one to isolate new elements of secondary structure, and reveals pronounced symmetry in the folding of secondary elements in the native globule.

EXPERIMENTAL

***Sm* nuclease.** The isoform *Sm* 1 was used, which lacks the first three residues (Asp-Thr-Leu) of the complete form *Sm* 2 [6, 7]. However, residue numbering was for the *Sm* 2 form, i.e., the N-terminal Glu of *Sm* 1 was designated as Glu4, and so on. Preliminary purification of the enzyme from its commercial preparation of M grade (NPO Vector, Novosibirsk) was carried out as described previously [6, 9].

Crystallization and collection of high-resolution diffraction data. The crystals used in high-resolution X-ray crystallographic analysis were obtained by hanging-drop free-interface diffusion. The starting solution contained 10–12 mg/ml protein, 0.6 M ammonium sulfate, 10 mM Tris-HCl (pH 8.3) and 5 mM $MgSO_4$. Prismatic crystals of 0.7 × 0.3 × 0.2 mm size were used in diffraction studies.

0026-8933/99/3302-0180$22.00 © 1999 МАИК "Наука/Interperiodica"

Diffraction data were collected using synchrotron radiation at the EMBL X11 station (c/o DESY, Hamburg) from a DORIS accumulating circle. An Imaging Plate detector of D. Hendriks and A. Lentfer was used. The diffraction data were integrated using the program DENZO (Z. Otwinowski).

RESULTS

The X-ray crystallographic parameters of *Sm* nuclease crystals and of the collected diffraction data are listed in Tables 1 and 2.

A PDB-deposited model refined earlier [11] at 2.1 Å resolution (29,466 reflections with $F/\sigma > 2$ at 6 to 2.04 Å) to an R factor of 16.8% was used as a starting model for the refinement. The model contained 3694 nonhydrogen atoms belonging to two protein molecules related by noncrystallographic symmetry, and 224 water molecules. The standard crystallographic R factor calculated for the whole data set (55,952 reflections with $F/\sigma > 2$ at 6 to 1.7 Å) was 32.4%. As water molecules are generally the least reliably determined part of the structure and the cell dimensions used in this work (Table 1) and by Miller *et al.* (106.7 × 74.5 × 68.9 Å)[11] differed somewhat, which might indicate differences in the water shell, all water molecules were removed from the starting model and reconstructed independently later. The removal of water molecules did not affect the initial value of the R factor, which was 36.0% in this case.

A control data set containing 10% of reflections randomly selected at the very beginning of the refinement was used to calculate R [12]. It should be noted that the same control set was used throughout the refinement and that the absolute values of structural factors for this set were used in neither model refinement nor in obtaining Fourier syntheses subsequently used for manual model corrections or water addition.

To decrease the noise in Fourier syntheses caused by neglecting the control set of the reflections in synthesis calculations, the absolute values of the structural factors calculated for the model were used in synthesis calculations. To decrease the noise associated with errors in the used phases of the structural factors, weight factors were introduced in the synthesis calculations. The factors were determined by maximizing the marginal likelihood function obtained from the control reflection set [13, 14].

The first stages of the refinement were done on an IBM 486 PC using the program FROG [15, 16] allowing easy arbitrary division of the model into blocks treated as solids. During the refinement procedure, the number of the reflections and the degrees of freedom for the model were increased gradually. At first, the data set was limited to 3.0 Å resolution for both molecules found in the asymmetric unit. Then the model was divided into two rigid groups composed of the main chain atoms of each molecule and rigid groups corresponding to each of the side chains. The refinement was increased to 2.1 Å. At the next stage, the resolution was increased to 1.9 Å, and the number of the

Table 1. X-Ray diffraction data for *Sm* nuclease crystals

Number of crystals	1
Space group	$P2_12_12$
Cell dimensions, Å:	
a	106.7
b	74.8
c	69.0
Number of molecules per asymmetric unit	2
Resolution, Å	30.3–1.7
Number of measured reflections ($I > \sigma$)	219270
Number of independent reflections ($I > \sigma$)	57095
Completeness, %	94.6
R_{merge}, %	7.0
R_{st}, %	5.3

Note: $R_{merge} = \Sigma|I-\langle I\rangle|/\Sigma\langle I\rangle$, $R_{st} = \Sigma\ \sigma/\Sigma\ I$, where I is measured reflection intensity and $\langle I\rangle$ is average intensity for symmetry-related reflections.

Table 2. Data collection statistics

Resolution, Å	Number of independent reflections	Number of measured reflections	Completeness, %
30.3–7.18	883	474	53.7
7.18–5.24	1355	1186	87.5
5.24–4.33	1686	1432	84.9
4.33–3.77	1957	1723	88.0
3.77–3.38	2200	2038	92.6
3.38–3.10	2411	2307	95.7
3.10–2.87	2596	2506	96.5
2.87–2.69	2784	2684	96.4
2.69–2.54	2945	2855	96.9
2.54–2.41	3110	3016	97.0
2.41–2.30	3260	3182	97.6
2.30–2.20	3400	3312	97.4
2.20–2.12	3540	3436	97.1
2.12–2.04	3664	3557	97.1
2.04–1.97	3788	3678	97.1
1.97–1.91	3935	3814	96.9
1.91–1.85	4041	3900	96.5
1.85–1.80	4163	4018	96.5
1.80–1.75	4252	4100	96.4
1.75–1.70	4392	3877	88.3

Table 3. Refinement statistics

Resolution, Å	6.0–1.7
Number of reflections used in refinement	50268
Number of control reflections not used in refinement	5679
Number of residues in model	2 × 239
Number of non-H atoms	3678
Number of water molecules	443
Standard *R* factor	17.3
Free *R* factor	22.2
Rms/maximal deviations for:	
Bonds, Å	0.011/0.069
Angles, deg	1.8/10.9
Average/maximal values of *B* factor (residues 7–243):	
Mainchain atoms, Å^2	12.9/31.4
Sidechain atoms, Å^2	16.0/50.5
Water molecules, Å^2	35.1/62.9
Average value of *B* factor (terminal residues 5–6 and 244-245):	
Mainchain atoms, Å^2	39.1
Sidechain atoms, Å^2	43.8
Distribution of dihedral angles on Ramachandran map, %	
In allowed regions	91.2
In additional allowed regions	7.8

degrees of freedom was increased by assuming each peptide group and each side chain to be an independent rigid group. Finally, all atoms of the model were refined separately, resulting in a 1.7 Å resolution. All stereochemical parameters (bond lengths, valent angles, planarity of particular atom groups, noncovalent interactions) not fixed in the rigid groups were controlled at all steps of the refinement. The resulting model was characterized by the crystallographic factors *R* of 24.1% and R_{free} of 29.2%; the average deviations of bond lengths and valent angles from their standard values were 0.004 Å and 1.06°, respectively.

Next, a two-step automatic procedure was used to add 358 water molecules to the model. First, about 2000 most intense peaks on the difference Fourier synthesis were selected and, second, their atomic neighborhood was analyzed, allowing identification of those water molecules which can H-bond to suitably placed neighboring atoms. The selection was done with the program ASIR [17].

Further refinement was carried out with the program X-PLOR [18]. At this stage, automatic refinement alternated with the analysis and interactive correction of the model with the programs FRODO [19] and O [20] implemented on graphic stations. At the final refinement steps, further water molecules were added by the above procedure so that their total number became 439 and the individual values of their refined *B* factors did not exceed 63 Å^2. The final values of the *R* and R_{free} factors for the resolution zone of 6.0–1.7 Å were found to be 17.3 and 22.2%, respectively. The average deviations of bond lengths and valent angles in the refined model were 0.011 Å and 1.8°, and their maximal values were below 0.07 Å and 11°, respectively. Inspection of the model with PROCHECK [21] has indicated that it is within the normally occurring range according to all considered parameters. Some characteristics of the refined structure are presented in Table 3.

DISCUSSION

According to the final model of *Sm* nuclease calculated with PROCHECK, the values of the torsion angles φ and ψ for the main chain are found in the allowed regions and all non-Gly residues adopt most favorable or allowed conformations. The model satisfies all the stereochemical requirements generally applied to high-resolution structures. The residues Ala10 and Asn177 are involved in γ-turns, which are nowadays also considered to be allowed conformations [24]. It should be noted that Ala10 is located in a short loop Cys-Ala-Val-Gly-Cys stabilized by an S–S bridge between the Cys residues and by the hydrogen bonds (Cys9)O...N(Val11), (Val11)O...N(Gly221), and (Gly12)O...N(Ala220). As indicated by a statistical analysis [25], Asn residues are more often found in

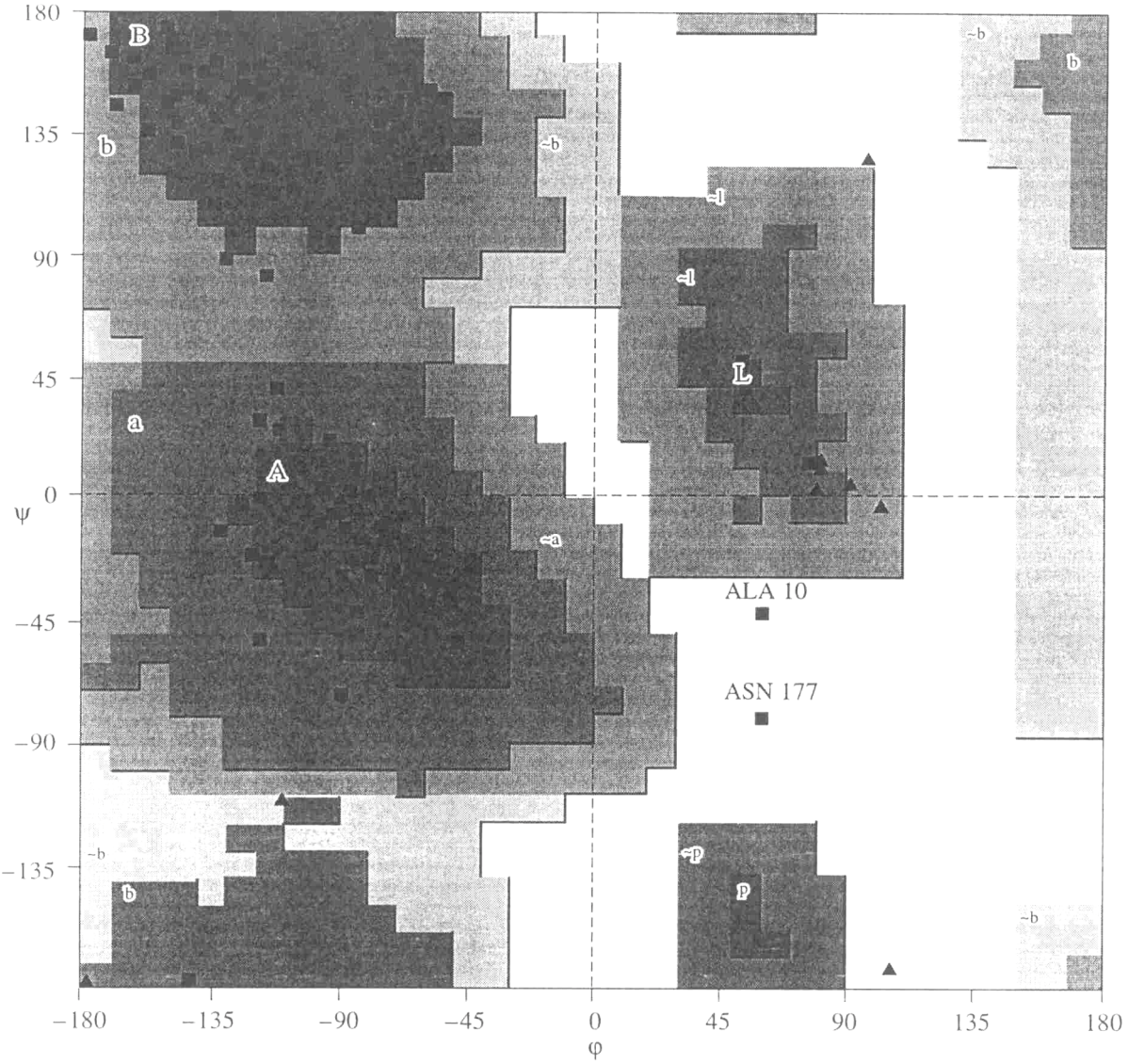

Fig. 1. A Ramachandran map for the refined structure of *Sm* nuclease.

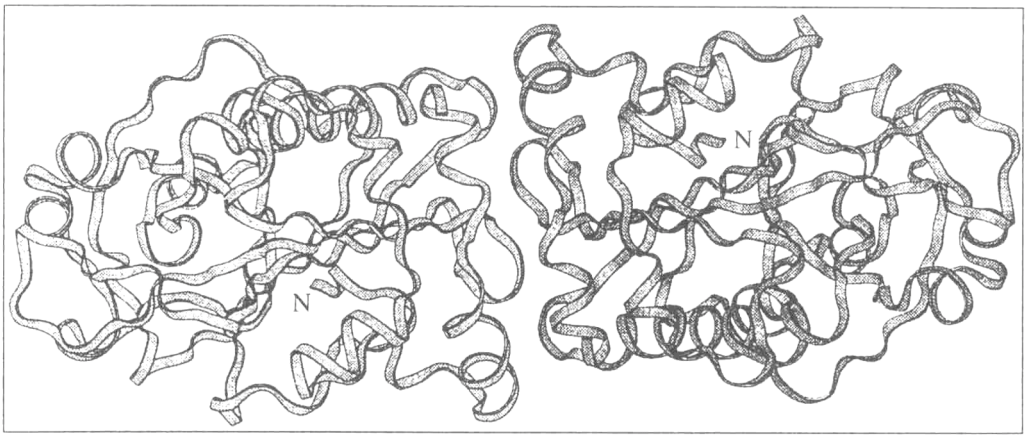

Fig. 2. The structure of *Sm* nuclease dimer refined to 1.7 Å resolution.

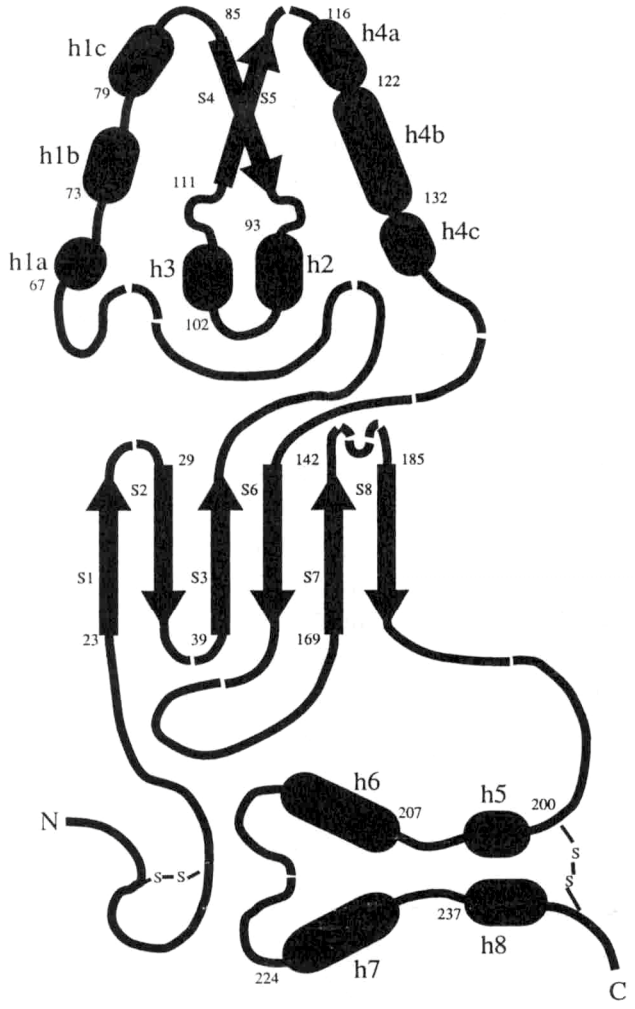

Fig. 3. A topological diagram of polypeptide chain in *Sm* nuclease at 1.7 Å resolution.

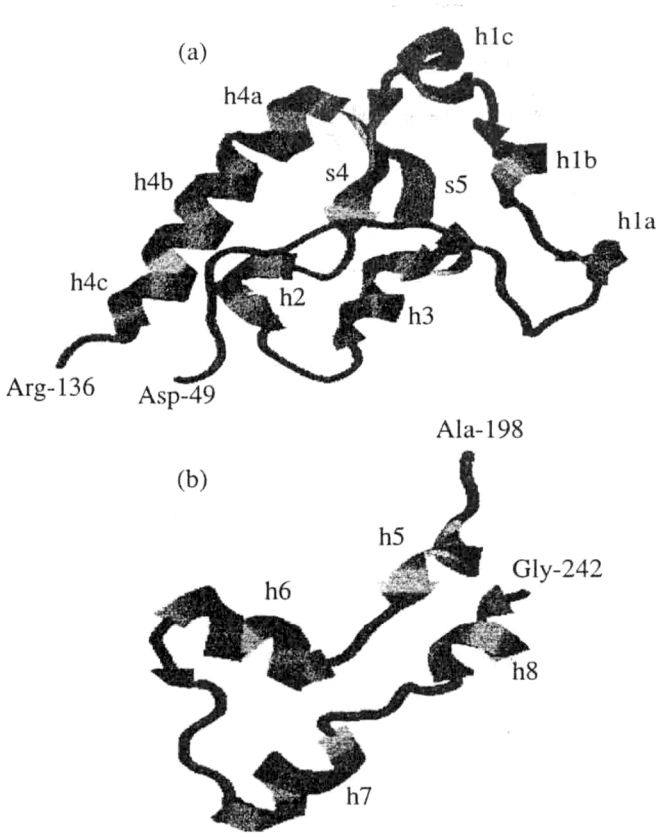

Fig. 4. The spatial arrangement of secondary structure elements at the N- and C-termini of *Sm* nuclease molecule.

the right part of the Ramachandran map than other residues.

Comparison of the final (Fig. 2) and starting [11] models of the *Sm* nuclease structure confirms the high quality of the starting model, which is not principally different from the final one. The root-mean-square difference in atom coordinates was 0.16 Å for the main chain atoms and 0.36 Å for all nonhydrogen atoms. Maximal differences (up to 0.75 Å for main chain atoms and 6.3 Å for side chain atoms) were observed in outer loops exposed to solution, and were characterized by high values of temperature factors. Similar differences were found when comparing two independently refined molecules located in the asymmetric unit and related by noncrystallographic symmetry: the rms and maximal differences in atom coordinates were 0.12 Å and 0.68 Å for the main chain atoms and 0.62 Å and 5.08 Å for the side chain atoms, respectively.

The structure of *Sm* nuclease refined to 1.7 Å suggests a topological scheme for the polypeptide chain (Fig. 3) different from that used previously [11]. This scheme reveals marked symmetry of separate loci in the globule.

The suggested modifications mainly concern two regions: the segment Asp49–Arg136 forming the upper layer of the molecule and participating in active site formation and substrate binding [11], and the C-terminal segment Ala198–Gly242 participating in dimer formation [26]. In the earlier structure, the polypeptide chain Asp49–Arg136 was considered to be a "long irregular loop Thr50–Gln114 followed by a long bent helix Lys115–Asp135" [11]. According to the present data, the visual inspection of the molecule (Fig. 2), the analysis of the distribution of the dihedral angles φ and ψ (Fig. 1), and the hydrogen bond network (Table 4) indicate that this region adopts a rigid enough conformation with an appreciable number of additional secondary structure elements (Fig. 4a).

The central part of the upper layer is formed by a double-stranded β-sheet s4 (Val85–His89), twisted through 180°, and s5 (Ile111–Lys115), embraced by a symmetrical system of helical fragments. The three

Table 4. Hydrogen bonds in fragments Asp49–Arg136 and Asp199–Gly242 of *Sm* nuclease main chain

Mainchain atoms		Distance, Å	Mainchain atoms		Distance, Å
Loop end stabilization			Helix, h4b		
Thr–50 O	Gly–98 N	2.8	Gly–121 O	Arg–125 N	3.0
Ala–52 N	Ala–94 O	3.0	Ala–122 O	Leu–126 N	3.0
Lys–60 N	Asn–106 O	3.3	Trp–123 O	Glu–127 N	3.0
Lys–60 O	Leu–108 N	3.0	Ala–124 O	Asp–128 N	3.0
Helix h1a			Arg–125 O	Gln–129 N	3.1
Asn–66 O	Asp–69 N	2.9	Leu–126 O	Glu–130 N	2.9
Pro–67 O	Thr–70 N	3.6	Glu–127 O	Arg–131 N	3.1
Helix h1b			Asp–128 O	Lyd–132 N	3.1
Ala–72 O	Asp–75 N	2.9	Helix h4c		
Pro–73 O	Tyr–76 N	3.2	Glu–130 O	Leu–133 N	3.2
Ala–74 O	Thr–77 N	3.2	Arg–131 O	Ile–134 N	3.4
Helix h1c			Lys–132 O	Asp–135 N	3.0
Gly–78 O	Ala–82 N	3.1	Helix h5		
Ala–79 O	Leu–83N	2.9	Asp–199 O	Gln–202 N	3.2
Asn–80 O	Lys–84 N	2.8	Phe–200 O	Phe–203 N	3.0
β-Strand s4–s5			Cys–201 O	Arg–204 N	3.6
Lys–84 O	Ser–116 N	2.9	Helix h6		
Asp–86 N	Gln–114 O	2.8	Thr–206 O	Ile–210 N	3.5
Asp–86 O	Gln–114 N	3.0	Val–207 O	Glu–211 N	3.0
Gly–88 N	Thr–112 O	3.0	Asp–208 O	Lys–212 N	2.9
Gly–88 O	Thr–112 N	3.1	Glu–209 O	Arg–213 N	3.1
Gln–90 N	Asn–112 O	2.9	Ile–210 O	Thr–214 N	3.0
Helix h2			Glu–211 O	Gly–215 N	2.9
Leu–93 O	Leu–96 N	3.2	Helix h7		
Leu–96 O	Val–99 N	3.1	Pro–223 O	Gln–227 N	3.1
			Asp–224 O	Ala–228 M	2.9
Helix h3			Asp–225 O	Ser–229 N	3.1
Asp–101 O	Ser–104 N	3.1	Val–226 O	Leu–230 N	2.9
Trp–102 O	Leu–105 N	2.9	Gln–227 O	Lys–231 N	3.1
Glu–103 O	Asn–106 N	3.0	Helix h8		
Ser–104 O	Tyr–107 N	3.1	Val–236 O	Glu–239 N	3.1
Helix h4a			Leu–237 O	Leu–240 N	2.9
Lys–115 O	Leu–118 N	3.0	Pro–238 O	Met–241 N	2.9
Lys–115 O	Asn–119 N	3.0	Glu–239 O	Gly–242 N	3.6
Ser–116 O	Asn–119 N	3.2			
Ser–116 O	Gln–120 N	2.9			
Asp–117 O	Gln–121 N	3.3			
Leu–118 O	Gln–121 N	3.2			
Leu–118 O	Trp–123 N	3.2			

short helices h1a (Pro67–Asp69, 3_{10} helix), h1b (Pro73–Tyr76, 3_{10} helix) and h1c (Ala79–Leu83, α-helix), preceding the β-sheet resemble in their spatial arrangement the helical region Ser116–Asp135, which is also formed by three adjacent helices h4a (Ser116–Gln120), h4b (Ala122–Arg131) and h4c (Lys132–Asp135) located at small angles to one another. The helix h4a is intermediate between 3_{10} and

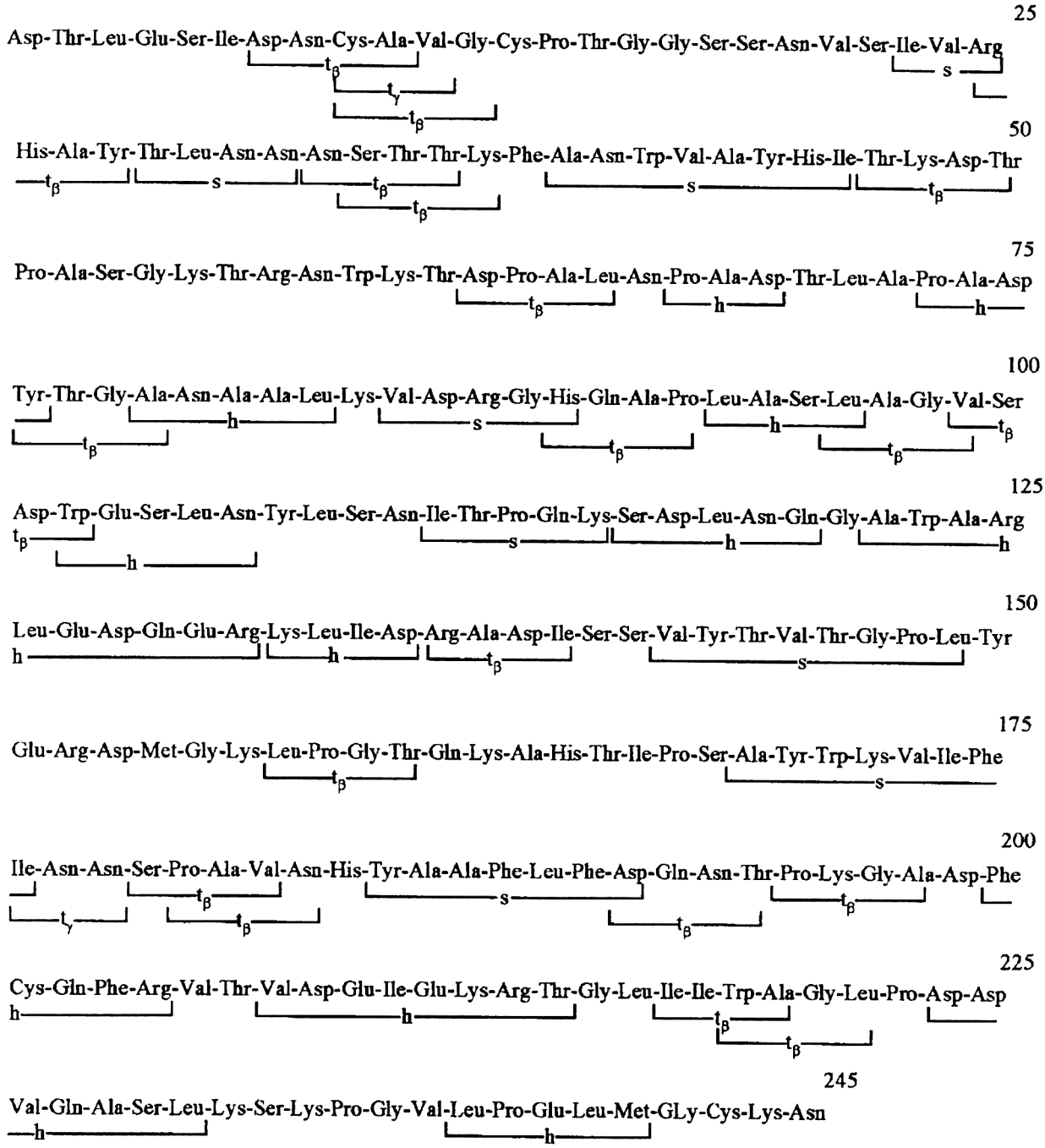

Fig. 5. The amino acid sequence of *Sm* nuclease and distribution of secondary structure elements: helices (h), β-structures (s), β- and γ-turns (t_β and t_γ) according to the 1.7 Å structure.

α-helix, h4b is a nearly ideal α-helix, and the terminal part of h4c is closer to 3_{10} helix. The strands ends with His89 and Ile111, which are connected by a arc formed by two short 3_{10} helices h2 (Leu93–Leu96) and h3 (Trp102–Asn106). The loop Thr50–Lys60 is in a nearly extended conformation and is H-bonded at its ends to helices h2 and h3. It should be noted that the entire Pro73–Asp135 chain is nearly planar and the Thr50–Lys60 chain forms a pin perpendicular to the plane. It is likely that the Thr50–Lys60 region, possessing a greater conformational freedom owing to the lack of stabilizing H-bonds, undergoes changes as the enzyme binds the magnesium ion and substrate.

The identification of a short previously unrecognized [11] helix h5 (Phe200–Arg204) in the C-termi-

nal part of the polypeptide chain Ala198–Gly242 reveals more clearly the inherent symmetry of this region (Fig. 4b). The symmetry is emphasized by the observation that the longer helices h6 (Val207–Thr214) and h7 (Asp224–Leu230) are α-helices, whereas the less ordered short helices h5 and h8 (Leu237–Met241) are closer to 3_{10} helices. The extensive structural symmetry of this region and of those discussed above in the nuclease molecule might result from duplication with inversion of the corresponding gene parts during evolution.

Additional ordered elements found in the 1.7 Å structure of *Sm* nuclease are β- and γ-turns, in which the polypeptide chain changes its direction by 180° (Fig. 5).

In conclusion, it may be noted that *Sm* nuclease is the second sugar-independent enzyme, after *Staphylococcus* nuclease, whose structure has been solved at a high resolution. However, the two nucleases differ in the specificity of phosphodiester bond hydrolysis (the staphylococcal nuclease splits 5' O-P bonds), are structurally dissimilar, and show mutually exclusive metal ion requirements (the staphylococcal nuclease is activated by Ca^{2+}), clearly indicating that the structure and mechanism of *Sm* nuclease are unique. In the next paper, we consider the active site organization and the catalytic mechanism of *Sm* nuclease.

ACKNOWLEDGMENTS

The authors are grateful to A.G. Urzhumtsev, N.L. Lunina, S.V. Nikonov, N.A. Nevskaya, A. Dementiev, A. Antson, Z. Dauter, and K.S. Wilson for the aid in this work and helpful discussions. Model analysis was done using the programs RasWin (R. Sayle) and PC MAGE (R.M. Weiss and D.C. Richardson). This work was supported by the International Science Foundation, projects MG9000 and MG9300, and the Russian Foundation for Basic Research, project nos. 94-04-12844, 97-04-48319 and 97-04-49772.

REFERENCES

1. Filimonova, M.N., Baratova, L.A., Vospel'nikova, N.D., Zheltova, A.O., and Leshchinskaya, I.B., *Biokhimiya*, 1981, vol. 46, pp. 1660–1665.
2. Vincent, R.D., Hofman, T.J., and Zassenhaus, H.P., *Nucl. Acids Res.*, 1988, vol. 16, pp. 3297–3312.
3. Zassenhaus, H.P. and Denniger, G., *Curr. Genet.*, 1994, vol. 25, pp. 142–149.
4. Cote, J. and Ruiz-Carriro, A., *Science*, 1993, vol. 261, pp. 765–769.
5. Muro-Pastor, A.M., Kuritz, T., Flores, E., Herrero, A., and Wolk, C.P., *J. Bacteriol.*, 1994, vol. 76, pp. 1093–1098.
6. Filimonova, M.N., Dementiev, A.A., Leshchinskaya, I.B., Bakulin, G.Yu., and Shlyapnikov, S.V., *Biochemistry* (Moscow), 1991, vol. 56, pp. 508–520.
7. Pedersen, J., Filimonova, M., Roepstorff, P., and Biedermann K., *Biochim. Biophys. Acta*, 1993, vol. 1202, pp. 13–21.
8. Bannikova, G.E., Blagova, E.V., Varlamov, V.P., Morgunova, E.Yu., Dementiev, A.A., and Shlyapnikov, S.V., *Bioorg. Khim.*, 1990, vol. 16, pp. 1678–1682.
9. Bannikova, G.E., Blagova, E.V., Dementiev, A.A., Morgunova, E.Yu., Mikhailov, A.M., Shlyapnikov, S.V., Varlamov, V.P., and Vainshtein B.K., *Biochem. Int.*, 1991, vol. 23, pp. 813–822.
10. Miller, M.D., Benedik, M.J., Sallivan, M.C., Shipley, N.S., and Krause, K.L., *J. Mol. Biol.*, 1991, vol. 222, pp. 27–30.
11. Miller, M.D., Tanner, J., Alpaugh, M., Benedik, M.J., and Krause, K.L., *Nature Struct. Biol.*, 1994, vol. 1, pp. 461–468.
12. Brunger, A.T., *Nature*, 1992, vol. 355, pp 472–474.
13. Lunin, V.Yu. and Skovoroda, T.P., *Acta Cryst.*, 1995, vol. A51, pp. 880–887.
14. Urzhumtsev, A.G., Skovoroda, T.O., and Lunin, V.Yu., *J. Appl. Cryst.*, 1996, vol. 29, pp. 741–744.
15. Urzhumtsev, A.G., Lunin, V.Yu., and Vernoslova, E.A., *J. Appl.Cryst.*, 1989, vol. 22, pp. 500–506.
16. Ivanov, M.E. and Urzhumtsev, A.G., *Joint CCP4 and ESF-EACBM Newsletter on Protein Crystallography*, 1995, vol. 31, pp. 20–22.
17. Tong, H., Guillemette, J.G., Mauk, A.G., Smith, M., and Brayer, C.D., *J. Appl. Cryst.*, 1994, vol. 27, pp. 421–426.
18. Brunger, A.T., *X-PLOR Manual*, New-Haven: Yale University Press, 1988.
19. Jones, T.A., *J. Appl. Cryst.*, 1978, vol. 11, pp. 268–272.
20. Jones, T.A., Zou, J.Y., Cowan, S.W., and Kjeldgaard, M., *Acta Cryst.*, 1991, vol. A47, pp. 110–119.
21. Lastowski, R.A., MacArthur, M.W., Moss, D.S., and Thronton, J.M., *J. Appl. Cryst.*, 1993, vol. 26, pp. 283–291.
22. Rose, G.D., Gierasch, L.M., and Smith, J.A., *Adv. Prot. Chem.*, 1985, vol. 37, pp. 1–109.
23. Milner-White, E.J., Ross, B.N., Ismail, R., Belhadj-Mastefa, K., and Poet, R., *J. Mol. Biol.*, 1988, vol. 204, pp. 777–782.
24. Hutchinson, E.G. and Thornton, J.M., *Prot. Sci.*, 1996, vol. 5, pp. 212–220.
25. Bosharov, M.A., *Biofizika*, 1997, vol. 42, pp. 753–764.
26. Miller, M.D. and Krause, K.L., *Prot. Sci.*, 1996, vol. 5, pp. 25–34.